nature neuroscience

Neural compensation in older people with brain amyloid-β deposition

Jeremy A Elman[1,3], Hwamee Oh[2,3], Cindee M Madison[2], Suzanne L Baker[1], Jacob W Vogel[2], Shawn M Marks[2], Sam Crowley[2], James P O'Neil[1] & William J Jagust[1,2]

Recruitment of extra neural resources may allow people to maintain normal cognition despite amyloid-β (Aβ) plaques. Previous fMRI studies have reported such hyperactivation, but it is unclear whether increases represent compensation or aberrant overexcitation. We found that older adults with Aβ deposition had reduced deactivations in task-negative regions, but increased activation in task-positive regions related to more detailed memory encoding. The association between higher activity and more detailed memories suggests that Aβ-related hyperactivation is compensatory.

Many people experience declining episodic memory ability with advancing age, a symptom that is also common in the early stages of Alzheimer's disease (AD). Although the cause of AD is unknown, current theories implicate brain accumulation of Aβ peptide as a very early event in AD pathogenesis[1]. Many older people who maintain normal cognitive function have been found at subsequent autopsy to harbor extensive Aβ plaque pathology, and more recent studies using PET imaging agents that bind to Aβ plaques have confirmed this observation *in vivo*[2–4]. The combination of declining memory and Aβ plaque deposits in normal older people suggests that these individuals may be in a preclinical phase of AD[5].

How do some older individuals maintain normal cognition in the face of Aβ deposition, while others succumb to cognitive decline and dementia? Functional magnetic resonance imaging (fMRI) studies of cognitively normal older people with brain Aβ deposition[6,7] and those with mild cognitive impairment (MCI)[8] have reported increased neural activity during cognitive activity in comparison to that in young people or older people without Aβ. However, the question of whether these Aβ-related increases are beneficial or harmful remains unresolved. We sought to address this question by adopting an fMRI task that probed the richness of each encoded stimulus by evaluating how the amount of memory detail was related to the extent of fMRI activation[9].

We studied 22 healthy young subjects and 49 cognitively normal older people (see **Table 1** and **Supplementary Table 1** for full subject characteristics). Using PET imaging with the amyloid imaging agent [^{11}C]Pittsburgh compound B (PIB), we split the older subjects into a group of 33 with no evidence of brain Aβ (PIB−) and a group of 16 with brain Aβ deposition (PIB+) on the basis of whole-brain PIB retention as measured with a distribution volume ratio and defined as the PIB index (see Online Methods for details). During the acquisition of fMRI data, subjects studied pictures of scenes and were told that they would later be asked questions about these stimuli (**Supplementary Fig. 1a**). Approximately 15 min after scanning, subjects were first tested for their memory of the central meaning of the stimuli ('gist memory'). Subjects viewed a set of written descriptions of scenes and were asked whether each corresponded to a previously studied picture or not (**Supplementary Fig. 1b**). Following this phase, subjects were required to respond whether each of six written details associated with each studied scene was true or false, giving a measure of memory richness (**Supplementary Fig. 1c**). The fMRI analyses assessed brain activations during encoding for items subsequently remembered during the gist task (hits) in comparison to baseline, as well as linear increases or decreases in activity related to the number of details remembered. To distinguish relative increases and decreases from baseline, we masked the results of these comparisons with task-positive and task-negative network maps derived from comparing hits to baseline averaged across all groups (**Fig. 1a**).

All groups performed significantly above chance on both gist and details tasks, with no between-group differences (**Table 1**). While young subjects scored better on multiple neuropsychological tests than the old groups, there were no differences between the PIB+ and PIB− groups (see **Supplementary Tables 1** and **2**). Across all participants, brain regions that were more active during encoding for gist hits resembled the previously described task-positive network[10], while areas that were deactivated included large regions of a task-negative network commonly referred to as the default mode network[11] (**Fig. 1a** and **Supplementary Table 3**). Brain regions that showed a parametric increase of activity related to the number of details recalled across groups were largely a subset of the regions activated during gist encoding, while areas exhibiting parametric decreases comprised a subset of the default mode network (**Fig. 1b** and **Supplementary Table 4**). Brain Aβ in old PIB+ individuals was characteristically deposited throughout medial and lateral association cortex, as well as medial frontal cortex (**Fig. 1c**).

While the primary focus of this study was to assess parametric changes in activity related to memory strength, results of the gist task were broadly consistent with previous findings. Both young and PIB+ individuals demonstrated greater activation for hits compared to baseline within task-positive regions in comparison to PIB− subjects (see **Supplementary Fig. 2** and **Supplementary Table 5**). In contrast, both groups demonstrated reduced deactivations for hits in task-negative regions. When hits were compared to misses, however, greater relative deactivations did occur in task-negative regions for young subjects (**Supplementary Fig. 3**).

[1]Life Sciences Division, Lawrence Berkeley National Laboratory, Berkeley, California, USA. [2]Helen Wills Neuroscience Institute, University of California, Berkeley, Berkeley, California, USA. [3]These authors contributed equally to this work. Correspondence should be addressed to J.A.E. (jelman@berkeley.edu) or W.J.J. (jagust@berkeley.edu).

Received 10 June; accepted 14 August; published online 14 September 2014; doi:10.1038/nn.3806

Table 1 Group characteristics

	Old PIB+	Old PIB−	Young
N	16	33	22
Age	75.56 (4.68)	76.82 (5.32)	23.64 (2.04)
Gender	7 male	13 male	11 male
Education (years of school)	16.37 (2.28)	16.67 (1.71)	15.95 (1.25)
APOE ε4 carriers/noncarriers	6/8	5/28	NA
Gist hit rate	0.71 (0.11)	0.67 (0.11)	0.64 (0.13)
Gist correct rejection rate	0.77 (0.15)	0.82 (0.09)	0.82 (0.12)
Gist sensitivity *d′*	1.40 (0.40)	1.40 (0.32)	1.37 (0.40)
Detail accuracy (per trial)	3.30 (0.19)	3.25 (0.19)	3.37 (0.25)
PIB index	1.22 (0.15)	0.99 (0.05)	NA
MMSE	28.56 (1.37)	28.85 (1.37)	NA

Values in parentheses are s.d. All groups performed similarly on both gist and detail tasks. Sensitivity *d′* = Z(hit rate) − Z(false alarm rate). MMSE, mini-mental state exam; NA, not applicable.

To assess parametric effects, we compared linear increases and decreases of activity across the number of details correctly identified for items remembered on the gist task between groups. The test of age effects compared young and old PIB− subjects, controlling for performance (gist hit rate) and voxelwise gray matter volume. Young subjects showed greater detail-related parametric increases than old PIB− subjects throughout lateral and ventral occipital cortex, superior and medial parietal cortex, and inferior temporal cortex (**Fig. 2a** and **Supplementary Table 6**). Examining these contrasts using the task-positive and task-negative masks from all participants revealed that most of these differences were due to greater increases in activity with more details remembered within task-positive areas in young subjects (**Fig. 2b**). While old PIB− individuals demonstrated relatively little modulation in task-positive regions, they showed greater deactivation with more recalled details in medial parietal cortex, a part of the task-negative network, as compared to young subjects (**Fig. 2c**). These findings indicate that when young people showed more activation than old for recall of the gist, the extent of activation contributed to forming richer and more detailed memories, while old subjects showed these effects for deactivation.

We similarly compared old PIB+ and PIB− subjects to examine the effect of amyloid on parametric increases in encoding activity. Old PIB+ subjects showed stronger parametric effects than PIB− subjects in parietal and occipital cortex, particularly in the right hemisphere (**Fig. 2d** and **Supplementary Table 6**). PIB+ individuals showed greater increases in brain activation across superior and lateral parietal as well as medial and lateral occipital cortex related to the number of details encoded (**Fig. 2e**). Old PIB− subjects again showed a minimal parametric response in task-positive regions, but greater linear decreases in task-negative regions, including right angular gyrus and medial parietal cortex, as more details were recalled (**Fig. 2f**). The PIB+ subjects showed relatively little linear decrease in these areas. The results were similar when PIB index was treated as a continuous variable rather than dichotomizing subjects into groups. That is, there were greater linear increases in task-positive lateral occipital cortex at higher levels of PIB index and reduced linear decreases in the task-negative medial parietal cortex (**Supplementary Fig. 4**). We also found that, among PIB+ individuals, the parametric increases apparent in task-positive regions were attenuated at the highest levels of amyloid accumulation (see **Supplementary Fig. 5**). It should be noted, however, that even these high-PIB subjects tended to show greater parametric increases than the PIB− group as a whole.

The parametric relationship between neural activity and memory richness is evidence that increased neural activity in those with brain Aβ is a beneficial process that reflects neural plasticity and serves a compensatory function. We also confirmed previous reports of reduced modulation of deactivation in PIB+ individuals[6], consistent with the idea that increased activation may also be related to this loss of deactivation in task-negative regions. Deposition of Aβ interferes with a variety of neural functions, including long-term potentiation[12], and induces aberrant local circuit properties[13]. Aβ is also associated with reduced task-positive network connectivity[14], and abnormal task-negative and task-positive network function could result in inefficient neural processes necessitating greater neural activity. Similar mechanisms have been proposed as a result of age-related changes[15,16] and could reflect the mechanism whereby older people with brain Aβ deposition are able to remain cognitively normal while those unable to recruit these resources decline.

Consistent with previous findings that hippocampal hyperactivity among MCI subjects appears to be detrimental[17], we did not find parametric increases of activity in the medial temporal lobe related to detailed memory formation. Thus, it is possible that previous reports of heightened hippocampal activity in individuals with amyloid deposition or more advanced MCI could reflect a different underlying mechanism[7] or a disease progression in which initial compensatory mechanisms begin to fail[18]. Indeed, we did find reduced parametric increases in subjects with the highest levels of amyloid deposition (**Supplementary Fig. 5**).

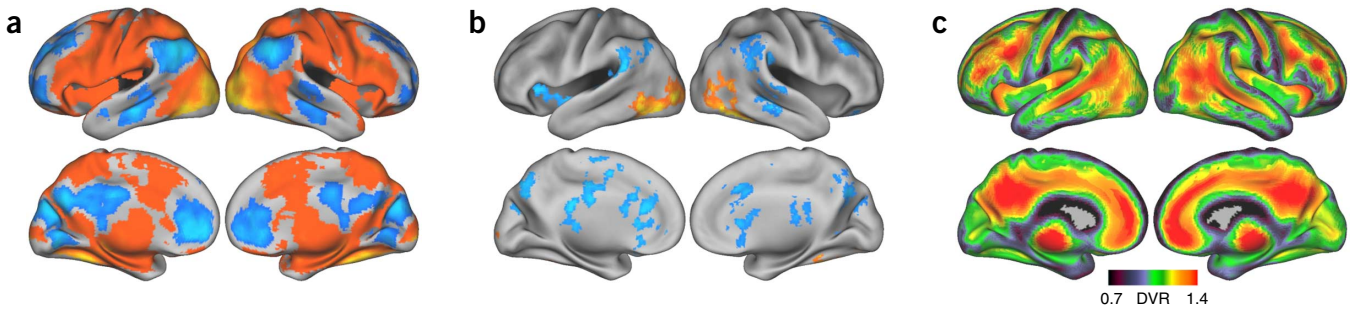

Figure 1 Group imaging results. Results are projected onto inflated atlas images. In each panel, lateral views are presented in top row and medial views in bottom row, with left hemisphere on the left and right hemisphere on the right. (**a**) Regions demonstrating encoding activation and deactivation related to successful gist memory (hits versus baseline) across all subjects. Warm colors indicate activation and cool colors indicate deactivation. (**b**) Regions demonstrating parametric encoding activation related to level of detail memory across all groups were defined by averaging the linear contrasts of gist hits classified by the number of correctly identified details. Warm colors indicate linear increases in brain activity with more details and cool colors indicate linear decreases. Results in **a**,**b** are thresholded at $P < 0.05$, cluster corrected for multiple comparisons. (**c**) A map of PIB binding in individuals demonstrating Aβ deposition was defined by averaging the PET images of subjects whose PIB index exceeded 1.07 (PIB+). Voxel values represent the distribution volume ratio (DVR; see Online Methods). Warm colors indicate higher Aβ deposition.

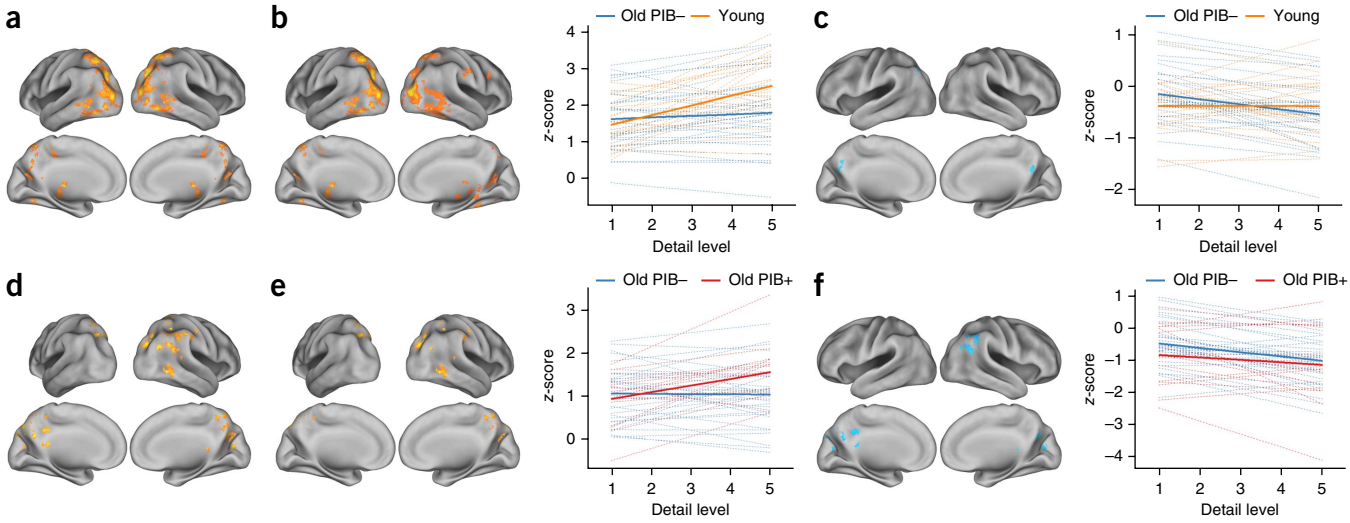

Figure 2 Age and Aβ effects on parametric encoding activity for details. Linear contrasts of activity related to number of details correctly recalled were assessed for age and PIB effects. Only items correctly remembered on the gist task were included. To distinguish between relative increases and decreases from baseline activity, tests of age (**a**) and PIB (**d**) were masked by the task-positive and task-negative networks (defined by contrasting hits with baseline, averaged across all groups) shown in **Figure 1a**. Plots displaying mean *z*-scores of significant clusters accompany masked results to better visualize underlying patterns of activity in the voxelwise analysis. Dashed lines represent subject-level linear regression lines and solid lines represent group estimates. (**a**) Greater linear increases in activity across detail level in young compared to old PIB– subjects (warm colors). (**b**) Task-positive regions show differences due to greater linear increases in young than PIB– subjects (warm colors). (**c**) Task-negative regions indicate greater linear decreases in PIB– subjects than young (cool colors). (**d**) Aβ effects revealed greater linear increases in old PIB+ compared to PIB– subjects (warm colors). (**e**) Task-positive regions indicate greater detail-related activation in old PIB+ than PIB– subjects (warm colors). (**f**) Task-negative regions show differences due to reduced detail-related deactivation in old PIB+ compared to PIB– subjects (cool colors). Results are thresholded at $P < 0.05$, cluster corrected for multiple comparisons.

The long-term consequences of brain Aβ deposition are still incompletely understood. It remains possible that individuals with brain Aβ and normal cognitive function are destined for eventual cognitive decline as neural inefficiency eventually increases to the point where compensation is no longer effective. In fact, this neural inefficiency itself may ultimately result in the deposition of increased Aβ, which is released through neural activity at the synapse[19,20]. The reduced parametric relationship between activation and performance in subjects with the highest levels of deposition (**Supplementary Fig. 5**) suggests that, at the very least, these regions make declining contributions to memory formation with continued amyloid accumulation. Whether and how individuals with brain Aβ can remain cognitively healthy for long periods of time is a question that will require longitudinal observation of behavior and neural function.

METHODS

Methods and any associated references are available in the online version of the paper.

Note: Any Supplementary Information and Source Data files are available in the online version of the paper.

ACKNOWLEDGMENTS

We thank S. Qin for task stimuli and W. Huijbers for discussion. Supported by US National Institutes of Health grant AG034570.

AUTHOR CONTRIBUTIONS

J.A.E., H.O. and W.J.J. designed the study; J.P.O. synthesized the [^{11}C]PIB; J.W.V. performed neuropsychological testing; S.C. performed PET acquisition; J.A.E. and H.O. performed MRI acquisition; S.L.B., C.M.M. and S.M.M. processed PET data; J.A.E., H.O. and C.M.M. processed MRI data; J.A.E. and H.O. analyzed data; J.A.E., H.O. and W.J.J. prepared the manuscript. J.A.E. and H.O. contributed equally to the study. All authors discussed results and commented on the manuscript.

COMPETING FINANCIAL INTERESTS

The authors declare no competing financial interests.

1. Jack, C.R. *et al. Lancet Neurol.* **12**, 207–216 (2013).
2. Bennett, D.A. *et al. Neurology* **66**, 1837–1844 (2006).
3. Morris, J.C. *et al. Ann. Neurol.* **67**, 122–131 (2010).
4. Aizenstein, H.J. *et al. Arch. Neurol.* **65**, 1509–1517 (2008).
5. Sperling, R.A. *et al. Alzheimers Dement.* **7**, 280–292 (2011).
6. Sperling, R.A. *et al. Neuron* **63**, 178–188 (2009).
7. Mormino, E.C. *et al. Cereb. Cortex* **22**, 1813–1823 (2012).
8. Dickerson, B.C. *et al. Ann. Neurol.* **56**, 27–35 (2004).
9. Qin, S., van Marle, H.J.F., Hermans, E.J. & Fernández, G. *J. Neurosci.* **31**, 8920–8927 (2011).
10. Naghavi, H.R. & Nyberg, L. *Conscious. Cogn.* **14**, 390–425 (2005).
11. Raichle, M.E. *et al. Proc. Natl. Acad. Sci. USA* **98**, 676–682 (2001).
12. Walsh, D.M. *et al. Nature* **416**, 535–539 (2002).
13. Palop, J.J. & Mucke, L. *Nat. Neurosci.* **13**, 812–818 (2010).
14. Oh, H. & Jagust, W.J. *J. Neurosci.* **33**, 18425–18437 (2013).
15. Morcom, A.M., Li, J. & Rugg, M.D. *Cereb. Cortex* **17**, 2491–2506 (2007).
16. Spreng, R.N., Wojtowicz, M. & Grady, C.L. *Neurosci. Biobehav. Rev.* **34**, 1178–1194 (2010).
17. Bakker, A. *et al. Neuron* **74**, 467–474 (2012).
18. O'Brien, J.L. *et al. Neurology* **74**, 1969–1976 (2010).
19. Cirrito, J.R. *et al. Neuron* **48**, 913–922 (2005).
20. Jagust, W.J. & Mormino, E.C. *Trends Cogn. Sci.* **15**, 520–526 (2011).

ONLINE METHODS

Participants. Seventy-four healthy elderly subjects underwent [^{11}C]PIB-PET and fMRI scanning and 31 young subjects underwent fMRI scanning for this study (see **Table 1** for subject characteristics). MRI scans were acquired within an average of 72 d of the PET scan (s.d. = 181.6 d, range = 0–1,263 d, median = 25 d). The subject with a delay of 1,263 d was strongly PIB+ and thus would be expected to remain in this group over time. All elderly subjects underwent a detailed battery of neuropsychological tests described previously[21]. All subjects were a subgroup of individuals who were recruited from the community via newspaper advertisements, talks at senior centers or word of mouth; young subjects were recruited from online subject registries. All subjects underwent a medical interview and a detailed battery of neuropsychological tests. To be eligible for the study, older subjects were required to be 65 years or older, live independently in the community without neurological or psychiatric illness, and have no major medical illness or medication that influenced cognition. All subjects' neuropsychological performance was within age-adjusted normal range (that is, within 1.5 s.d. of the mean scores). Although longitudinal follow-up data on these older subjects are not available yet, none of subjects reported cognitive symptoms at the time of participation. Apolipoprotein E (*APOE*) ε4 carrier status was determined for older subjects using previously published methods[22]. All subjects provided informed consent in accordance with the Institutional Review Boards of the University of California, Berkeley, and the Lawrence Berkeley National Laboratory (LBNL). Twenty-five elderly and 9 young subjects were excluded because of poor performance (<45% hit rate on the gist task; $N = 8$), problems with data collection (behavioral, MRI or PET; $N = 11$) or excessive motion ($N = 15$), resulting in a total number of 49 cognitively normal old and 22 young subjects for data analysis. Eight elderly and 1 young subject included in the present study participated in an experiment of episodic memory encoding previously published from our laboratory[7]. There were no significant differences between the groups in the number of subjects excluded for any of the above reasons.

Behavioral procedure. The memory task used here was adapted from Qin *et al.*[9]. Subjects completed a scanned encoding session during which 150 pictures of scenes were presented over 3 functional runs (**Supplementary Fig. 1**). Images were presented on a black background for 6.6 s, during which subjects responded whether there were people or no people in the scene with a button press using a four-button response box using either thumb (response mappings were counterbalanced across subjects). A white fixation cross then appeared for 1–4 scan repetition times (TRs) (mean inter-trial interval = 4 s) before moving on to the next trial.

Following a 15-min delay, the subsequent memory test phase took place outside the scanner on a desktop computer. This session was composed of two tasks that we refer to as the gist and details tasks, each split into 3 blocks. During the gist task, which lasted approximately 30 min, subjects were presented a total of 150 written descriptions of studied scenes, intermixed with 150 descriptions of unstudied scenes. Subjects were instructed to decide whether each description was associated with an old (presented during encoding) or new (not presented during study) scene, as well as their confidence in the response (high or low). During the details task, which lasted approximately 90 min, only memory for the 150 scenes presented at encoding was assessed. For each encoded item, subjects were first presented the associated gist description, followed by a set of 6 details related to the scene. Subjects were instructed to respond whether each detail was true or false. The number of true details varied randomly from 2 to 4 across trials. Responses were made with a key press and subjects were given a maximum of 10 s to respond for each item. The order of item presentation during the memory tests was varied randomly for each subject.

PIB-PET acquisition. [^{11}C]Pittsburgh compound B (PIB) was synthesized at the LBNL Biomedical Isotope Facility using a published protocol and described in detail previously[23]. PIB-PET imaging was performed at LBNL using an ECAT EXACT HR or BIOGRAPH Truepoint 6 scanner (Siemens Medical Systems, Erlangen, Germany) in three-dimensional acquisition mode. Approximately 15 mCi of PIB was injected into an antecubital vein. Immediately upon injection, dynamic acquisition frames were obtained as follows: 4 × 15 s, 8 × 30 s, 9 × 60 s, 2 × 180 s, 10 × 300 s and 2 × 600 s (90 min total). Ten-minute transmission scans for attenuation correction or X-ray CT were obtained for each PIB scan. PET data were reconstructed using an ordered subset expectation maximization algorithm with weighted attenuation. Images were smoothed with a 4-mm Gaussian kernel with scatter correction.

MRI acquisition. Subjects were scanned in a 1.5-T Magnetom Avanto (Siemens Medical Systems, Erlangen, Germany) scanner at LBNL. Each of the three functional runs were acquired with a T2*-weighted echo-planar imaging (EPI) sequence [TR = 2,200 ms; TE = 50; flip angle = 90°; matrix = 64 × 64; FOV = 220 mm; voxel size = 3.44 × 3.44 × 3.4 mm, duration = 9 min]. 28 axial slices oriented to the AC-PC were acquired in an interleaved order, giving whole brain coverage. Two hundred forty-six volumes were collected during each of the functional runs. The first five volumes of each run were discarded to allow for magnetization preparation. A high-resolution magnetization-prepared rapid-acquisition gradient echo (MPRAGE) image [TR = 2,110 ms; TE = 3.58 ms; matrix = 256 × 256; FOV = 256; sagittal plane; voxel size = 1 × 1 × 1 mm; 160 slices] and an in-plane turbo inversion recovery image [TR = 2,000 ms; TE = 11; matrix = 256 × 256; FOV = 220; voxel size = 0.9 × 0.9 × 3.4 mm, 28 slices] were collected for registration purposes.

PIB-PET processing. All PIB-PET data were preprocessed using SPM8 software[24]. The first five frames were summed, and all frames including the summed image were realigned to the middle (17th) frame. The subject's structural data were coregistered to their PIB-PET data using the mean image of frames corresponding to the first 20 min of acquisition as a target. PIB distribution volume ratio (DVR) images were created using Logan graphical analysis with frames corresponding to 35–90 min after injection and a gray matter (GM) cerebellum reference region defined using FreeSurfer v5.1 software[25–27]. Mean DVR values from frontal, parietal, temporal and cingulate cortices were computed to serve as a global PIB index for all older subjects.

Elderly subjects were dichotomized into PIB– and PIB+ groups on the basis of a cut-off defined from a group of 18 young subjects who received PIB-PET scans and showed no PIB retention. Eleven of these subjects were scanned on the ECAT HR and seven on the Biograph; the mean and s.d. for the global PIB DVRs were almost identical (ECAT: mean = 1.014, s.d. = 0.023; Biograph: mean = 0.993, s.d. = 0.036). These subjects were presumed to be Aβ free and provide a baseline level of absent PIB binding. Using a method previously reported[7], the PIB positivity cut-off was taken as 2 s.d. above the mean PIB index value of these young subjects (mean = 1.01, s.d. = 0.03), resulting in a value of 1.07. Experimenters were blinded to subjects' PIB status during data collection.

fMRI processing. fMRI data were preprocessed and analyzed with the FSL toolbox v5.0 (ref. 28). Motion correction was performed with MCFLIRT, aligning all images to the middle slice with rigid body transformation. Slice timing correction was performed using (Hanning windowed) sinc interpolation to shift each slice in the volume in reference to the middle of the TR period. BET (Brain Extraction Tool) was then used to create a mask of the brain from the first volume of each time series and used to separate brain from surrounding skull and tissue in each volume. All images were spatially smoothed with a 6-mm FWHM Gaussian kernel to reduce noise. High-pass temporal filtering was performed with a 100-s cut-off using the local Gaussian-weighted fit of a running line to remove low-frequency artifacts. Subject data were registered to standard space in a three-step process using FNIRT (FMRIB's Nonlinear Image Registration Tool). First, EPIs were linearly registered to each subject's skull-stripped, in-plane anatomical image. Second, the in-plane anatomical image was linearly registered to the skull-stripped high resolution T1-weighted image. Third, the subject's T1-weighted images were nonlinearly registered to standard space (FSL's MNI152 template). The three registrations were then combined to take the subject's EPI images and run-level statistical maps into standard space in one transformation. GM partial volume maps were generated using FSL's FAST tool in order to be included as voxelwise regressors controlling for atrophy. The smoothing of these maps was matched to that of the functional images after registration to standard space.

fMRI analysis. Individual runs from the encoding session were modeled in subject space using FSL's FEAT v6.0 tool, and resulting statistical maps were registered to standard space for higher level analysis. Separate models were generated for the gist and details tasks. For the gist model, trials were classified as hits or misses. Hits and misses were collapsed across confidence level to ensure a sufficient number of events per condition. In the details model, hits and misses

doi:10.1038/nn.3806

were further categorized by the number of details correctly recalled (for example, Hit_1, Miss_1, Hit_2, Miss_2). Regressors of interest were obtained by convolving stimulus onset times with FSL's double gamma hemodynamic response function and their temporal derivative. Motion parameters and outlier volumes (defined as excessive motion or intensity) were included as additional confound variables and temporal autocorrelation was removed through pre-whitening. A contrast of hits versus baseline was generated for the gist task to measure relative activations and deactivations for encoded items. A linear contrast was formed in the details model to assess activity parametrically modulated by the number of details encoded. Only trials classified as hits during the gist task were included, and detail levels 0–1 and 5–6 were combined to increase the number of events within these conditions. This resulted in linear contrast of [Hit_5+6 > Hit_4 > Hit_3 > Hit_2 > Hit_0+1].

A second level analysis combined these contrasts from the three runs for each subject using a one-sample *t*-test, treating runs as fixed effects. Third-level group statistics maps were created using the Robust Biological Parametric Mapping (rBPM) toolbox[29,30], treating subjects as a random factor. rBPM allows for the inclusion of voxelwise regressors and implements a robust regression model (using the bisquare weight function) to reduce sensitivity to outliers. Performance and GM partial volume maps were included as nuisance regressors, and the average was taken across all three groups. The age effect was assessed by comparing the young and old PIB– groups, including GM partial maps and performance (hit rate) as nuisance regressors. The PIB effect was assessed by comparing old PIB+ and old PIB– groups, including GM partial volume maps, performance (hit rate) and age as nuisance regressors. Performance was included to account for individual differences on the memory task and to account for varying numbers of hit trials included in contrasts across subjects. The whole-brain family-wise error was cluster corrected to $P < 0.05$ (two-sided) using a cluster forming threshold of $P < 0.05$. Thresholded statistical maps were projected on inflated atlases for display purposes using Caret v5.64 software[31]. The group comparisons do not distinguish between increased activation and reduced deactivation. Therefore, we examined the relative directionality of significant voxels by masking them with task-positive and task-negative network maps derived from comparing hits to baseline averaged across all groups (**Fig. 1a**). These masked results, as well as plots displaying average activity of significant clusters falling within each masked region, are presented for visualization purposes.

A **Supplementary Methods Checklist** is available.

21. Oh, H., Habeck, C., Madison, C. & Jagust, W. *Hum. Brain Mapp.* **35**, 297–308 (2014).
22. Agosta, F. *et al. Proc. Natl. Acad. Sci. USA* **106**, 2018–2022 (2009).
23. Rabinovici, G.D. *et al. Neurology* **68**, 1205–1212 (2007).
24. Friston, K.J., Ashburner, J.T., Kiebel, S.J., Nichols, T.E. & Penny, W.D. *Statistical Parametric Mapping: The Analysis of Functional Brain Images* (Academic, 2011).
25. Logan, J. *et al. J. Cereb. Blood Flow Metab.* **16**, 834–840 (1996).
26. Price, J.C. *et al. J. Cereb. Blood Flow Metab.* **25**, 1528–1547 (2005).
27. Dale, A.M., Fischl, B. & Sereno, M.I. *Neuroimage* **9**, 179–194 (1999).
28. Jenkinson, M., Beckmann, C.F., Behrens, T.E.J., Woolrich, M.W. & Smith, S.M. *NeuroImage* **62**, 782–790 (2012).
29. Casanova, R. *et al. Neuroimage* **34**, 137–143 (2007).
30. Yang, X., Beason-Held, L., Resnick, S.M. & Landman, B.A. *Neuroimage* **57**, 423–430 (2011).
31. Van Essen, D.C. *Neuroimage* **28**, 635–662 (2005).